Intestinal Activation of pH-Sensing Receptor OGR1 [GPR68] Contributes to Fibrogenesis

Hutter, Senta; van Haaften, Wouter T.; Huenerwadel, Anouk; Baebler, Katharina; Herfarth, Neel; Raselli, Tina; Mamie, Celine; Misselwitz, Benjamin; Rogler, Gerhard; Weder, Bruce

Published in:
Journal of Crohn's and Colitis

DOI:
10.1093/ecco-jcc/jjy118

Publication date:
2018

Journal of Crohn's and Colitis, 2018, 1348–1358
doi:10.1093/ecco-jcc/jjy118
Advance Access publication August 25, 2018
Original Article

Original Article

Intestinal Activation of pH-Sensing Receptor OGR1 [*GPR68*] Contributes to Fibrogenesis

Senta Hutter[a,#], Wouter T. van Haaften[b,c,#], Anouk Hünerwadel[a], Katharina Baebler[a], Neel Herfarth[a], Tina Raselli[a], Céline Mamie[a], Benjamin Misselwitz[a], Gerhard Rogler[a,d], Bruce Weder[a], Gerard Dijkstra[b], Chantal Florence Meier[a], Cheryl de Vallière[a], Achim Weber[f], Pedro H. Imenez Silva[d,e], Carsten A. Wagner[d], Isabelle Frey-Wagner[a], Pedro A. Ruiz[a], Martin Hausmann[a]

[a]Department of Gastroenterology and Hepatology, University Hospital Zürich, Zürich, Switzerland [b]Department of Gastroenterology and Hepatology, University Medical Center Groningen, University of Groningen, Groningen, The Netherlands [c]Department of Pharmaceutical Technology and Biopharmacy, Groningen Research Institute of Pharmacy, University of Groningen, Groningen, The Netherlands [d]Institute of Physiology, University of Zürich, Zürich, Switzerland [e]Kidney Control of Homeostasis, Swiss National Centre of Competence in Research, Zürich, Switzerland [f]Department of Pathology and Molecular Pathology, University Hospital Zürich, Zürich, Switzerland

[#]Equal contribution.

Corresponding author: Martin Hausmann PhD, Department of Gastroenterology and Hepatology, University Hospital Zürich, 8091 Zurich, CH-Switzerland. Tel: 41-44-255-9916; Fax 41-44-255-9496; Email: martin.hausmann@usz.ch

Abstract

Background and Aims: pH-sensing ovarian cancer G-protein coupled receptor-1 [OGR1/*GPR68*] is regulated by key inflammatory cytokines. Patients suffering from inflammatory bowel diseases [IBDs] express increased mucosal levels of OGR1 compared with non-IBD controls. pH-sensing may be relevant for progression of fibrosis, as extracellular acidification leads to fibroblast activation and extracellular matrix remodelling. We aimed to determine *OGR1* expression in fibrotic lesions in the intestine of Crohn's disease [CD] patients, and the effect of *Ogr1* deficiency in fibrogenesis.
Methods: Human fibrotic and non-fibrotic terminal ileum was obtained from CD patients undergoing ileocaecal resection due to stenosis. Gene expression of fibrosis markers and pH-sensing receptors was analysed. For the initiation of fibrosis *in vivo,* spontaneous colitis by *Il10*$^{-/-}$, dextran sodium sulfate [DSS]-induced chronic colitis and the heterotopic intestinal transplantation model were used.
Results: Increased expression of fibrosis markers was accompanied by an increase in *OGR1* [2.71 ± 0.69 vs 1.18 ± 0.03, $p = 0.016$] in fibrosis-affected human terminal ileum, compared with the non-fibrotic resection margin. Positive correlation between *OGR1* expression and pro-fibrotic cytokines [*TGFB1* and *CTGF*] and pro-collagens was observed. The heterotopic animal model for intestinal fibrosis transplanted with terminal ileum from *Ogr1–/–* mice showed a decrease in mRNA expression of fibrosis markers as well as a decrease in collagen layer thickness and hydroxyproline compared with grafts from wild-type mice.
Conclusions: *OGR1* expression was correlated with increased expression levels of pro-fibrotic genes and collagen deposition. *Ogr1* deficiency was associated with a decrease in fibrosis formation. Targeting OGR1 may be a potential new treatment option for IBD-associated fibrosis.

Key Words: Fibrosis; Crohn's disease; IBD models

1. Introduction

Recent studies have shown a link between inflammatory bowel diseases [IBDs] and the family of pH-sensing G-protein-coupled receptors [GPRs].[1–5] Three GPRs from the GPR4 subfamily were identified as sentinels for proton concentration, because they enable cells to sense the surrounding pH and to respond to it.[6,7] This GPR4 subfamily of receptors includes GPR4, ovarian cancer GPR 1 [OGR1/*GPR68*], and T cell death-associated gene 8 [TDAG8/*GPR65*]. These receptors sense extracellular protons through histidine residues located in the extracellular region of the receptors, resulting in signalling pathway activation and the modification of a variety of cell functions.[6,7] GPRs are also regulated by key inflammatory cytokines.[8–10] The proton-sensing pH receptors TDAG8, OGR1 and GPR4 are inactive or only slightly active in an alkaline environment [pH 7.6–7.8], but become highly activated in acidic environments [pH 6.8].[7,11–13] GPR132 structurally belongs to the same subclade, but is pH insensitive and therefore is not considered a pH-sensing GPR.[14]

IBD affects approximately 1 in 150 people in the industrialized world. It comprises two main conditions, namely ulcerative colitis [UC] and Crohn's disease [CD], and is characterized by a chronic inflammation of the intestinal wall. Severe and persistent mucosal tissue damage is one of the main features of IBD. Tissue injury is associated with an acidic pH shift, as inflammation increases the local proton concentration and lactate production.[15] This induces subsequent pro-inflammatory cytokine production, such as tumor necrosis factor [TNF].[15–17] An acidic environment is not only the result of inflammation, but also affects the degree and outcome of inflammation.[13,18,19] A disturbed pH homeostasis due to acidification of the intestinal environment leads to the activation of OGR1.[20] Recent work demonstrates that patients suffering from IBD express increased levels of *OGR1* in the mucosa compared with in non-IBD controls.[3,4] The expression of *OGR1* is also increased in inflamed colonic mucosa compared with non-inflamed colonic mucosa in both CD and UC patients. Moreover, in mice lacking *Ogr1*, inflammation is attenuated.[4]

Wound healing after tissue damage requires an exquisite balance between multiple pro- and anti-fibrotic stimuli on extracellular matrix [ECM]-producing cells[21–24] e.g. activated myofibroblasts.[25] Matrix-producing cells are activated by paracrine signals, autocrine factors, damage-associated molecular patterns, or pathogen-associated molecular patterns derived from microorganisms.[26–29] Transforming growth factor β1 [TGF-β1] is an important mediator of mesenchymal cell activation, and its expression is increased in the inflamed mucosa of IBD patients.[30–33] Excessive tissue repair promotes fibrosis, impairs gastrointestinal function, and is a common clinical problem in patients with CD and UC.[34] Increased tissue stiffness is associated with impaired absorption upon fibrogenesis.[29] Fibrosis is increasingly recognized as an important cause of morbidity and mortality in patients with IBD. Intestinal fibrosis leads to stricture formation due to thickening of the intestinal wall in 30–50% of patients with CD,[35,36] and ~80% of these patients will require surgery.[35] Recently, it has been shown that fibrogenesis can also occur in long-standing [≥10 years] UC, leading to the formation of strictures.[37]

In this study, we determined the expression of *OGR1* in fibrotic lesions of human intestine in patients with CD compared with non-fibrotic control sections. Our results showed that *OGR1* expression correlated with the expression of pro-fibrotic genes and the levels of collagen deposition. Furthermore, we studied the role of Ogr1 in intestinal fibrogenesis in three different animal models of intestinal fibrosis. Our results showed that *Ogr1* deficiency was associated with a decrease in fibrosis formation. Targeting *OGR1* may be a potential new treatment option for IBD-associated fibrosis.

2. Materials and Methods

2.1. Human tissue from patients with CD and non-fibrotic control patients

Intestinal tissue from patients with CD was obtained from patients undergoing ileocaecal resection because of stenosis in the terminal ileum [non–fibrosis-affected resection margin and from the thickened fibrosis-affected region], and from patients undergoing right-sided hemicolectomy because of an adenocarcinoma [non–cancer-affected ileal resection margin, Supplementary Table 1]. Just after resection, samples for RNA were fixed in Tissue-Tek® [O.C.T. Compound, Sakura® Finetek] in the operation room and frozen in isopentane on dry ice. Samples were stored at –80°C until further use. Intestinal epithelial crypts were isolated as previously described.[38]

2.2. Animals

All animal experiments were performed according to the ARRIVE criteria for *in vivo* experiments. The generation, breeding and genotyping of male C57BL/6J-Ogr1^{tm1} [*Ogr1*$^{-/-}$], initially obtained from Deltagen, Inc., San Mateo, CA, has been described previously.[4,20] The animals were co-housed to minimize any potential effects of different microbiota. The animals received standard laboratory mouse food and water *ad libitum*. They were housed under specific pathogen-free conditions in a regular day–night cycle in individually ventilated cages with standard bedding and cage enrichment.

For the model of spontaneous colitis *Il10*$^{-/-}$ [C57BL/6] mice and *Ogr1*$^{-/-}$ mice were crossed to generate *Ogr1*$^{-/-}$*/Il10*$^{-/-}$ colitis-susceptible mice. Female mice were observed until reaching 80 days of age.

Chronic colitis was induced as described previously.[39] During a cycle of chronic colitis, female mice received either 1.75% dextran sodium sulfate [DSS] in drinking water or drinking water alone over 7 days. In between cycles, the animals were given 14-day periods of recovery. Mice received three cycles of DSS treatment as described above and were euthanized 3 weeks after completion of the last DSS cycle.

For the model of heterotopic transplantation, male C57BL/6 wild-type [WT] donor mice were obtained from Jackson Laboratories; 12 female B6-Tg$^{UBC-GFP}$30Scha/J (ubiquitin C [UBC]–green fluorescent protein [GFP] recipient) mice were bred locally.

The mice used for all of the above-mentioned experiments weighed 19–23 g and were 11–16 weeks old when the experiment was started. Surgeries were always performed during the light cycle.

2.3. Ethical considerations

Patients gave written informed consent for anonymous use of patient data and resected parts of human intestine, according to the code of conduct for responsible use of surgical left-over material [see: Code goed gebruik voor gecodeerd lichaamsmateriaal, Research Code University Medical Center Groningen, www.rug.nl/umcg/research/documents/research-code-info-umcg-nl.pdf]. Further, we retrieved permission to isolate different mucosal cells from intestinal samples, and to use data from patients from a cohort study of Swiss residents diagnosed with IBD, approved by the local ethical committee of the Kanton Zurich [EK-1316]. The animal experiment protocol was approved by the Veterinary Authority of the Kanton of Zurich [registration number ZH242/2016].

2.4. Assessment of colonoscopy and histological score in mice

Animals were anaesthetized intraperitoneally with a mixture of 90–120 mg ketamine [Narketan 10%, Vétoquinol AG, Bern Switzerland] and 8 mg xylazine [Rompun 2%, Bayer, Switzerland]

per kilogram body weight, and examined with the Tele Pack Pal 20043020 [Karl Storz Endoskope, Germany]. Mice were scored with a murine endoscopic index of colitis severity [MEICS] as described previously.[40] For the assessment of the histological scores, 1 cm of the distal third of the colon was removed and scored as described.[39,41]

2.5. Heterotopic intestinal transplant model

The heterotopic mouse intestinal transplant model is an adaption of the heterotopic transplantation model of intestinal fibrosis in rats, which has been previously described in detail.[42] Briefly, donor small bowel resections were extracted and transplanted subcutaneously into the neck of recipient animals. Donor small bowel proximal to the caecum was excised and flushed with 5 mL of 0.9% NaCl to remove stool, and divided into 10 mm parts. A small bowel resection was implanted into a subcutaneous pouch, and a single dose of Cefazolin [Kefzol®, Teva Pharma AG 1 g diluted in 2.5 mL distilled water] was administered intraperitoneally as infection prophylaxis. Intestinal grafts were explanted 7 days after transplantation. Donor and recipient mice were euthanized by cervical dislocation. After explantation, each graft was divided into three equal segments. One segment was fixed in 4% formalin for histopathological assessment. The other two segments were snap frozen in liquid nitrogen and stored at –80°C until RNA extraction or for determination of hydroxyproline [HYP] content.

2.6. RNA isolation and RT-qPCR from Tissue-Tek–embedded samples and from mouse samples

For human samples, ten 10 µM-thick Tissue-Tek sections, containing full cross-sections of the intestinal wall were cut using a cryostat. Sections were dissolved and homogenized in TRIzol [Invitrogen, Life Technologies], and the total RNA was isolated according to the manufacturer's protocol. To avoid genomic DNA contamination, samples were treated with DNase I, Amp Grade [Invitrogen, Life Technologies] according to the manufacturer's protocol. RNA isolation from mucosa, crypts and epithelial cells was performed as previously described.[38] RNA isolation of mice specimens was performed following the instructions of the RNeasy Mini Kit [Qiagen]. RT-qPCR was performed using TaqMan gene expression assays [Supplementary Table 2]. mRNA expression is presented as $2^{-\Delta Ct}$, normalized to one of the samples in the control group.

2.7. Sirius Red staining and collagen layer thickness measurement

Fixed samples were processed in a benchtop tissue processor [Leica TP 1020], embedded and cut into 3-µm sections. To visualize the collagen layer, the samples were stained with Sirius Red according to a standard protocol.[43] Sirius Red staining was examined using the Imager Z2 microscope [Zeiss] and the software AxioVision [Zeiss]. The quantity of the Sirius Red–stained collagen was analysed by ImageJ 1.47t [NIH, USA] using pictures taken under transmission light, as well as using a polarized light filter. To quantify the area with Sirius red–stained collagen, cropped 100-fold magnification pictures [length:width ratio = 3:1] from at least eight representative areas comprising the collagen layer broadwise for each single graft were taken. By setting thresholds to select the red collagen using ImageJ, the area being covered with collagen was quantified. Additionally, collagen layer thickness was measured in micrometres by a blinded investigator in at least eight representative areas at 100-fold magnification.

2.8. 4-Hydroxyproline assay

HYP [a major component of collagen] content was quantified from freshly isolated small bowel and grafts using a HYP assay [MAK008-1KT, Sigma-Aldrich] according to the manufacturer's protocol. In brief, tissues [10–30 mg] were homogenized using gentleMACS Octo Dissociator [130-096-427, Miltenyl Biotec] and hydrolyzed in 12 M HCl [10 µL/mg tissue]. The hydrolysate was transferred in duplicates to a 96-well plate and dried at 60°C. Dried samples were incubated with 50 µL of chloramine T/oxidation buffer mixture [3 µL of the chloramine T concentrate and 47 µL of the oxidation buffer] at room temperature for 5 min. Single aliquots of 50 µL of the diluted DMAB reagent [25 µL dimethylaminobenzaldehyde, 25 µL perchloric acid/isopropanol] was added, and samples were incubated at 60°C for 90 min for chromophore formation. Absorbance was measured at 560 nm.

2.9. Statistical analysis

GraphPad Prism software [v5.0] was used. All human RT-qPCR data was considered non-parametric. Therefore, non-paired analyses were performed using the Mann–Whitney U test, and paired analyses were performed using a Wilcoxon matched-pairs signed rank test. If more than two groups were compared, a Kruskal–Wallis with *post-hoc* Dunn's test for multiple comparisons was performed. Correlation was determined using Spearman's rank correlation coefficient.

Statistical analysis for collagen layer thickness was performed using one-way analysis of variance on ranks, with pairwise correction for multiple comparisons [Student–Newman–Keuls method]. Statistical analysis for the HYP assay was performed using an unpaired *t*-test. Statistical analysis for RT-qPCR in mice was performed using an unpaired *t*-test or one-way analysis of variance on ranks, all pairwise multiple comparison procedures [Student–Newman–Keuls method].

Differences were considered significant at a p-value of <0.05 (indicated by an asterisk). In the text and figures, averages ± standard error of the mean are presented.

3. Results

3.1. Expression of *OGR1* was increased in fibrotic intestine from CD patients

To elucidate the pathophysiological relevance of pH-sensing receptors, we investigated whether the expression of GPRs was increased in fibrosis-affected terminal ileum vs non-fibrotic terminal ileum from patients with CD. Coincidentally, all included patients with CD were female. mRNA expression of fibrosis markers *COL1A1* [108.46 ± 60.57 vs 6.70 ± 2.02, $p < 0.05$], *COL3A1* [35.68 ± 17.66 vs 3.14 ± 0.73, $p < 0.05$], *ACTA2* [13.91 ± 4.10 vs 5.12 ± 2.20, $p < 0.04$], and *TGFB1* [4.72 ± 1.18 vs 1.52 ± 0.34, $p < 0.001$] was significantly increased in the fibrosis-affected area, compared with the non-fibrosis-affected resection margin [Figure 1A]. The increase in fibrosis markers was accompanied by a significant increase in the mRNA expression of *OGR1* [2.71 ± 0.69 vs 1.18 ± 0.03, $p < 0.05$] in the fibrosis-affected terminal ileum [Figure 1B]. To verify that the [unaffected] resection margins were free of fibrosis, we compared these samples with non-cancer-affected terminal ileum resection margins from resections due to adenocarcinoma. Here, no differences were observed in mRNA expression of *COL1A1* [5.78 ± 3.16 vs 4.40 ± 1.32, $p > 0.99$], *COL3A1* [1.67 ± 0.63 vs 2.00 ± 0.47, $p = 0.56$], *ACTA2* [4.47 ± 3.18 vs 1.58 ± 0.68, $p = 0.37$], and *TGFB1* [12.64 ± 8.96 vs 2.96 ± 0.84, $p = 0.37$, Supplementary

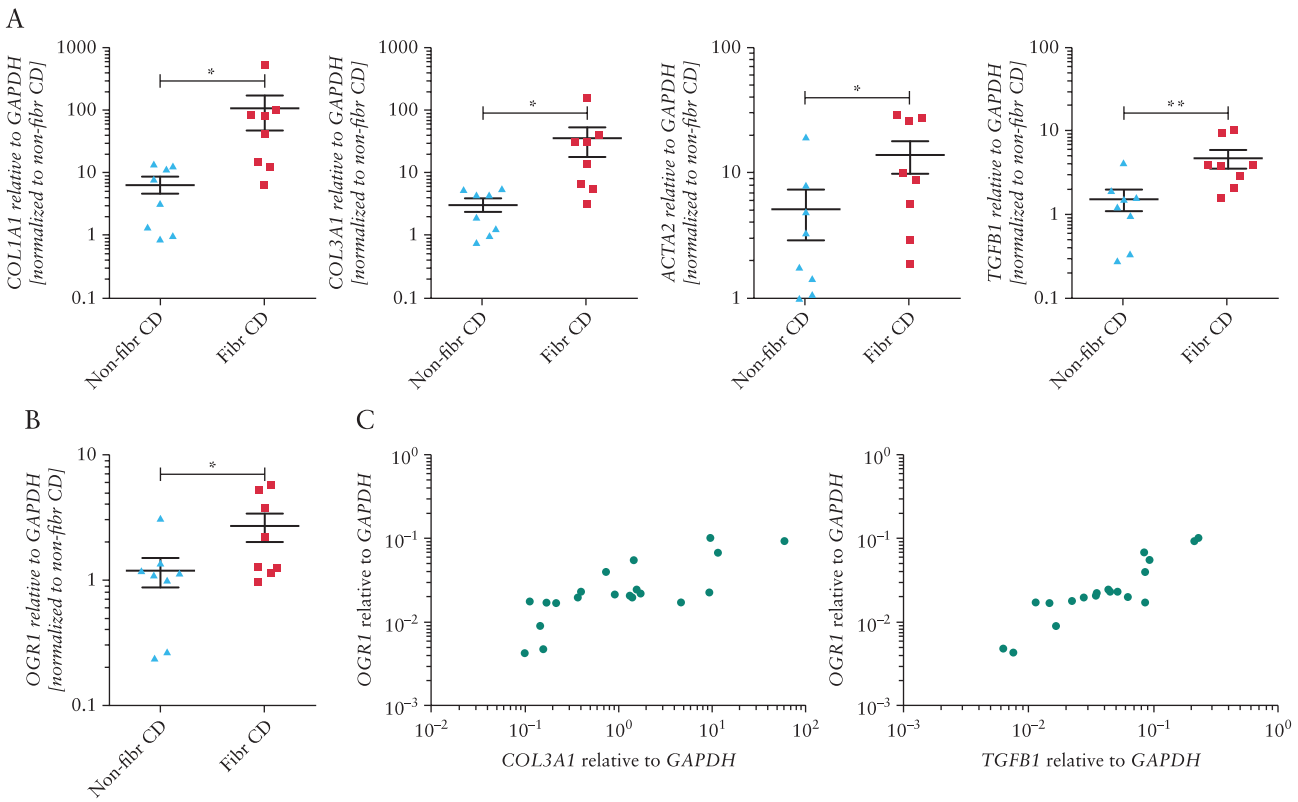

Figure 1. mRNA expression of fibrosis markers *COL1A1, COL3A1, ACTA2, TGFB1* [**A**] and G-protein coupled receptor [GPR] *OGR1* [**B**] in fibrotic versus non-fibrotic terminal ileum of patients with CD [by Wilcoxon matched-pairs signed rank test]. [**C**] Positive correlation in mRNA expression between *OGR1* vs *COL3A1* [$\rho = 0.791$, $p < 0.001$] and *TGFB1* [$\rho = 0.791$, $p < 0.01$] [by Spearman's rank correlation coefficient].

Figure 1A]. Also, no differences were observed between non-cancer-affected control tissue and the non-fibrosis-affected resection margin from patients with CD in *OGR1* [18.41 ± 0.16.17 vs 1.23 ± 0.33, $p = 0.56$, Supplementary Figure 1B]. Furthermore, a positive linear correlation between *OGR1* vs *COL3A1* [$R^2 = 0.791$, $p < 0.001$] and *TGFB1* [$R^2 = 0.850$, $p < 0.001$] was found [Figure 1C, Table 1]. This confirmed our hypothesis that expression of *OGR1* was associated with fibrogenesis in human terminal ileum, affected by CD.

To further examine which cells of the intestinal mucosa express the pH-sensing receptor, mRNA expression for *OGR1* was determined in RNA isolated from epithelial cells and mucosa from the same patient sample [Supplementary Figure 2]. mRNA expression was increased in whole mucosal tissue compared with in isolated crypts for *OGR1* [15.7 ± 15.0 vs 1.2 ± 2.5, $p < 0.01$, Supplementary Figure 2]. These results suggested that *OGR1* is mainly expressed by non-epithelial cells of the *lamina propria* of the human intestine such as immune cells or vascular cells.

3.2. Decreased fibrosis in *Ogr1*-deficient mice following spontaneous colitis

We hypothesized that increased expression of pH-sensing receptor OGR1 plays a role in fibrosis formation in both human and murine intestine. To investigate whether OGR1-dependent changes have functional consequences during fibrogenesis, three different murine models were used. First, the *Il10*$^{-/-}$ model of spontaneous colitis was used. Regarding inflammatory parameters, *Ogr1*$^{-/-}$*/Il10*$^{-/-}$ mice showed less lymphocyte accumulation in the intestinal mucosa, and a decreased prolapse ratio and MPO level compared with

Table 1. Spearman correlation between markers of fibrosis and *OGR1*.

		OGR1
COL1A1	Correlation coefficient	0.791
	p value	0.000
COL3A1	Correlation coefficient	0.779
	p value	0.000
ACTA2	Correlation coefficient	0.689
	p value	0.001
TGFB1	Correlation coefficient	0.850
	p value	0.000

Ogr1$^{+/+}$*/Il10*$^{-/-}$ mice, as recently published.[4] There were no differences in colon length, relative spleen weight, or in mRNA expression levels of the pro-inflammatory cytokines *Tnf*, *Il6*, or *Ifn*γ. Concerning fibrosis parameters, *Col3a1*, *Vim*, *Ctgf*, and *Tgfb1* were used to determine the level of fibrosis in this model, and to study the effect of the lack of *Ogr1*. Here, we could demonstrate that mRNA expression of *Col3a1* was significantly decreased in *Ogr1*$^{-/-}$*/Il10*$^{-/-}$ mice compared with in *Ogr1*$^{+/+}$*/Il10*$^{-/-}$ mice [0.51 ± 0.1 vs 1.0 ± 0.15, $p < 0.001$, Figure 2A], showing that fibrosis was reduced upon the absence of *Ogr1*. A trend for decreased mRNA expression of *Vim*, a mesenchymal cell marker that can be used as a surrogate marker for the number of fibroblasts and the occurrence of endothelial-to-mesenchymal transition [EMT], in *Ogr1*$^{-/-}$*/Il10*$^{-/-}$ mice [$p = 0.06$], together with *Ctgf* [$p < 0.02$] and *Tgfb1* [$p < 0.27$, Figure 2A], was observed.

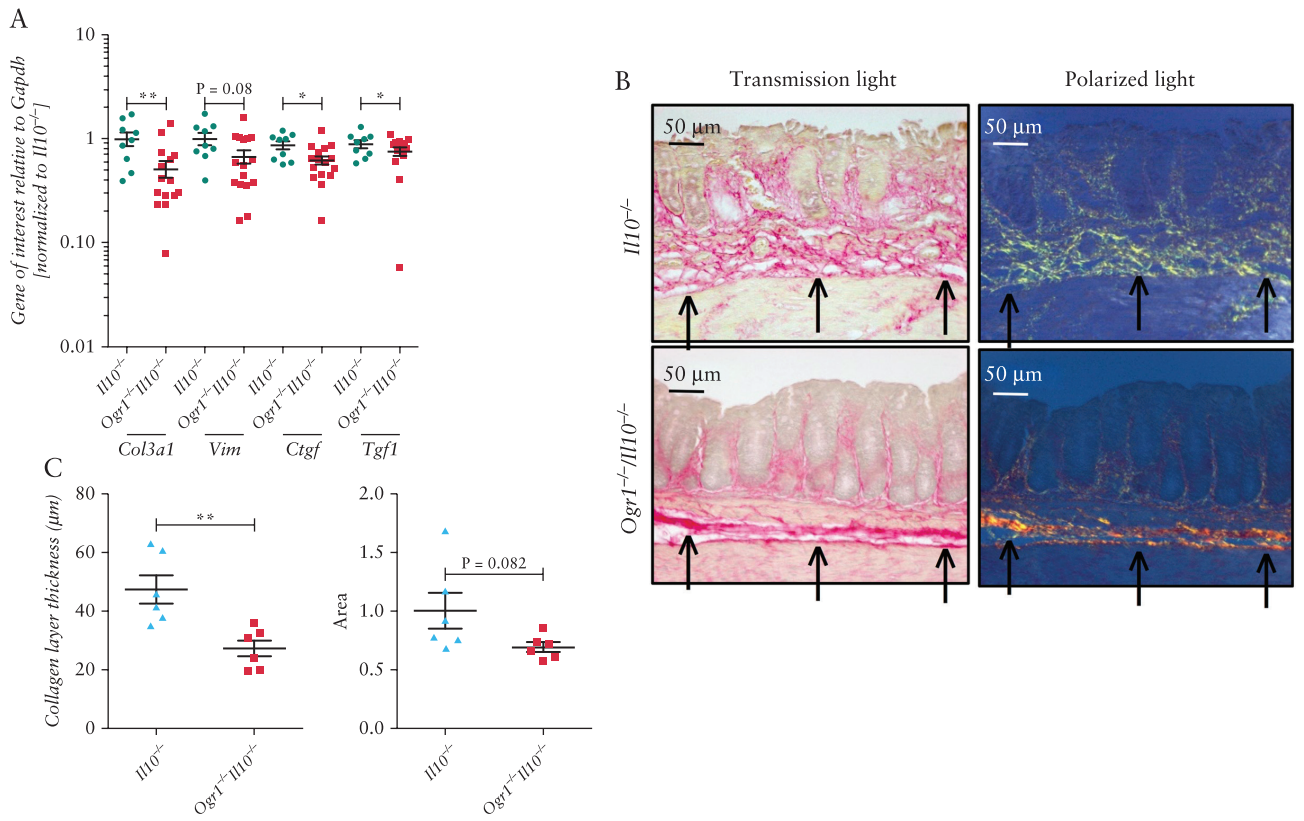

Figure 2. Collagen quantity and collagen layer thickness are decreased in colon from *Ogr1*$^{-/-}$/*Il10*$^{-/-}$ double knockout mice compared with *Il10*$^{-/-}$ mice following onset of spontaneous colitis. *Col3a1*, *Vim*, *cTgf*, and *Tgf* mRNA expression is decreased in colon from *Ogr1*$^{-/-}$/*Il10*$^{-/-}$ mice compared with *Il10*$^{-/-}$ mice [each by unpaired *t*-test, **A**]. Representative pictures of collagen deposition [arrows] visualized using Sirius Red staining with and without polarized light [**B**]. Quantification of collagen layer thickness [µm] by Sirius Red staining without polarized light filter [C, by unpaired *t*-test]. Quantification of collagen deposition by Image J software [by unpaired *t*-test, C].

To determine changes in ECM deposition, we performed Sirius Red staining to assess collagen deposition. Ogr1$^{+/+}$/Il10$^{-/-}$ mice with spontaneous colitis displayed a prominent collagen layer thickness in the colon [Figure 2B]. Increased short-chain collagen [green stain] was observed in the mucosa as a sign of an ongoing fibrotic process. In contrast, collagen deposition was significantly decreased in *Ogr1*$^{-/-}$/*Il10*$^{-/-}$ mice compared with in *Ogr1*$^{+/+}$/*Il10*$^{-/-}$ mice [27 ± 2.9 vs 47 ± 4.9, $p < 0.001$, Figure 2C]. Microscopy evidence indicated that long-chain collagen [red stain] was associated with a thinner collagen layer as a sign of lower accumulation of newly synthesized collagen.

Collagen deposition in the grafts was, furthermore, quantified by image-processing evaluation [color threshold] with ImageJ. Here, a non-significant trend for decreased collagen deposition in the *Ogr1*$^{-/-}$/*Il10*$^{-/-}$ mice was observed compared with in the *Ogr1*$^{+/+}$/*Il10*$^{-/-}$ mice [0.69 ± 0.04 vs 1.0 ± 0.15, $p = 0.08$, Figure 2C].

3.3. Decreased fibrosis in *Ogr1*-deficient mice with DSS-induced chronic colitis

For a second experimental approach, we used the DSS-induced chronic colitis model. We investigated whether absence of *Ogr1* reduces fibrosis in the model of DSS-induced chronic colitis [$n = 25$ mice]. Successful induction of colitis was confirmed by an intermittent body weight loss and a significant increase in spleen weight [data not shown]. *Ogr1*$^{-/-}$ was efficacious in ameliorating colitis, confirmed by a decreased MEICS and a decreased histological score [Figure 3A] compared with WT. DSS-induced thickening of the colon appeared to be increased because organs behind the bowel wall were no longer visible through the colon tissue. In contrast, in chronic colitis a reduced thickening of the colon appeared in *Ogr1*$^{-/-}$ compared with WT mice (0.81 ± 0.79 [$n = 8$] vs 1.25 ± 0.69 [$n = 6$], $p < 0.30$, Figure 3A and B), suggesting reduced fibrogenesis and ECM deposition. DSS-treated mice suffering from chronic colitis displayed a prominent collagen layer thickness in the colon [Figure 3C]. The fibrosis parameters *Col1a1*, *Col4a1*, and *Mmp9* were used to determine the level of fibrosis in this model, and to study the effect of the lack of *Ogr1*. Here we demonstrated that mRNA expression of *Col4a1* was significantly decreased in *Ogr1*$^{-/-}$ mice compared with in WT mice (1.06 ± 0.22 [$n = 8$] vs 1.55 ± 0.57 [$n = 6$], $p < 0.05$ Figure 3D), showing that fibrosis was reduced upon the absence of *Ogr1*. *Col3a1*, *Vim*, *Ctgf*, and *Tgfb1* remained unchanged [not shown]. Collagen deposition was decreased in *Ogr1*$^{-/-}$ compared with WT mice as determined by collagen layer thickness in the colon (1.01 ± 0.25 [$n = 8$] vs 1.42 ± 0.64 [$n = 6$], $p < 0.05$, Figure 3E) and HYP assay (0.27 ± 0.09 [$n = 8$] vs 0.37 ± 0.10 [$n = 6$], $p = 0.081$, Figure 3F).

3.4. Expression of pH-sensing receptors increased upon fibrogenesis in the heterotopic transplant model for intestinal fibrosis

To confirm the relevance of OGR1 in fibrogenesis in a third murine model, *Ogr1*$^{-/-}$ and WT mice were used as donors, and GFP-expressing mice as recipients for isogeneic transplantation of the intestine in the heterotopic animal model for intestinal fibrosis.

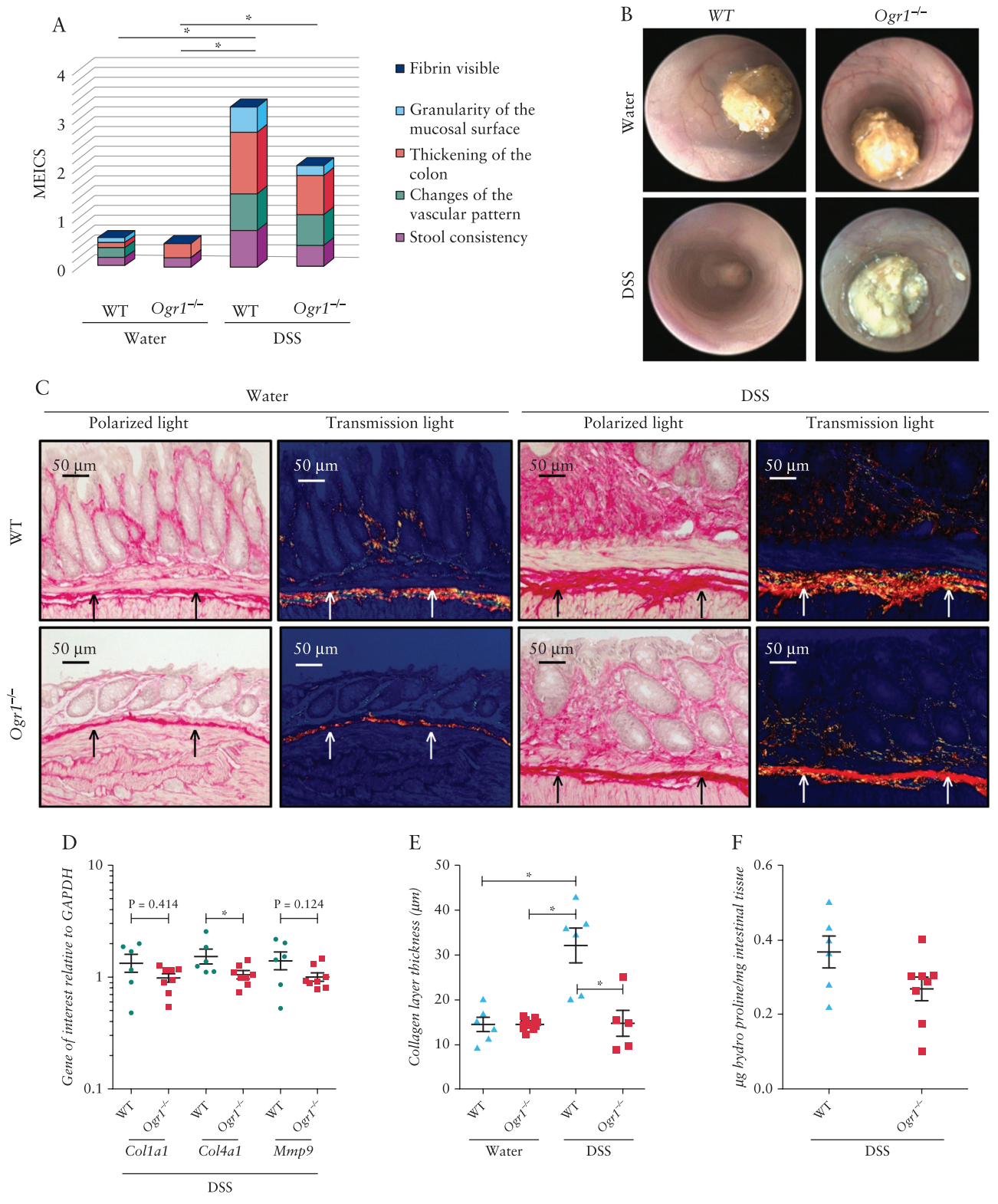

Figure 3. Collagen quantity and collagen layer thickness are decreased in colons from *Ogr1*$^{-/-}$ mice compared with WT mice upon DSS-induced chronic colitis. Mucosa from mice without DSS-induced colitis displayed a smooth and transparent mucosa with a normal vascular pattern and a solid stool. After induction of colitis, the colon of WT mice appeared with a thickened and more granular mucosa without stool, compared with *Ogr1*$^{-/-}$ mice with a clear vascular pattern, improved transparency, and loose stool. WT animals exhibited a higher MEICS score compared with *Ogr1*$^{-/-}$ mice after DSS treatment [**A**]. Coloscopy, representative images [**B**]. Representative pictures of collagen deposition [arrows] visualized using Sirius Red staining with and without polarized light [**C**]. There is a trend towards a decrease in *Col1a1*, *Col4a1*, and *Mmp9*mRNA expression in colon from *Ogr1*$^{-/-}$ mice compared with WT [each by unpaired *t*-test, **D**]. Quantification of collagen layer thickness [µm] by Sirius Red staining without polarized light filter [**E**, by ANOVA *post-hoc* Newman–Keuls multiple comparison test]. Quantification of collagen deposition by HYP assay [by unpaired *t*-test, **F**].

Body weight remained unchanged in both GFP recipient groups receiving either *Ogr1*$^{-/-}$ or WT grafts [data not shown]. Grafts were explanted 7 days after transplantation. From the 24 intestinal transplants, histologically evaluable tissue was obtained from all but five grafts: two WT and three *Ogr1*$^{-/-}$ mice. *Ogr1* mRNA expression in intestinal explants from WT donor mice on Day 7 after heterotopic transplantation was indeed significantly increased compared with in WT donor grafts on Day 0 before transplantation [5.71 ± 1.03 vs 1.92 ± 0.72, $p < 0.05$, Figure 4A].

3.5. HYP content was significantly decreased in *Ogr1*$^{-/-}$ grafts

Formation of HYP, an amino acid playing a key role in the stability of collagen, was determined in explanted grafts from mice on Day 7 after heterotopic transplantation. HYP content was significantly decreased in grafts from *Ogr1*$^{-/-}$donor mice compared with in grafts of WT donor mice after heterotopic transplantation [0.12 ± 0.02 vs 0.31 ± 0.04, $p < 0.001$, Figure 4B]. This result confirmed that collagen deposition, as well as collagen stability, was reduced upon *Ogr1* depletion in this murine model of intestinal fibrosis.

3.6. Expression of fibrosis markers was decreased in *Ogr1*$^{-/-}$ grafts upon induction of fibrosis

Expression of fibrosis markers *Vim*, *Col3a1*, *Tgfb1*, and *Ctgf* was used to confirm the induction of fibrosis in this model and to study the effect of the lack of *Ogr1*. *Vim* was increased in WT grafts 7 days after transplantation compared with in the small bowel at Day 0 [4.94 ± 0.85 vs 0.65 ± 0.08, $p < 0.001$, Figure 4C]. Furthermore, mRNA expression of *Col3a1* [395.55 ± 201.0 vs 1.15 ± 0.17, $p < 0.05$], *Tgfb1* [4.75 ± 0.94 vs 0.98 ± 0.17, $p < 0.001$], as well as *Ctgf* [8.08 ± 2.63 vs 1.70 ± 0.64, $^{*}p < 0.05$, Figure 4D–F] was increased in grafts from WT donor mice 7 days after transplantation, showing that fibrosis was adequately induced in this model. mRNA expression of these four markers was not significantly increased in the *Ogr1*$^{-/-}$ grafts 7 days after heterotopic transplantation, compared with in the small bowel on Day 0 [Figure 4C–F].

A non-significant trend for decreased *Vim* expression in freshly isolated small bowel and from *Ogr1*$^{-/-}$ compared with WT mice was observed [Figure 4C]. The expression of *Col3a1* mRNA was also decreased in *Ogr1*$^{-/-}$ grafts compared with in WT mice on Day 7 after transplantation [76.55 ± 28.88 vs 395.55 ± 201.0 $p < 0.05$, Figure 4C]. Furthermore, mRNA expression of *Tgfb1* and *Ctgf*, two mediators involved in activation of myofibroblasts, was significantly decreased in *Ogr1*$^{-/-}$ grafts on Day 7 compared with in WT grafts [*Tgfb1*: 2.33 ± 0.47 vs 4.75 ± 0.94, $p < 0.01$, Figure 4E; *Ctgf*: 3.12 ± 0.59 vs 8.08 ± 2.63, $p < 0.05$, Figure 4F]. In summary, markers of fibrogenesis are significantly decreased in *Ogr1*$^{-/-}$ grafts compared with in WT grafts in this heterotopic transplantation model for intestinal fibrosis. Fibrosis was successfully induced in this model in the WT grafts, whereas the expression of fibrosis markers remained unchanged in the *Ogr1*$^{-/-}$ grafts after heterotopic transplantation.

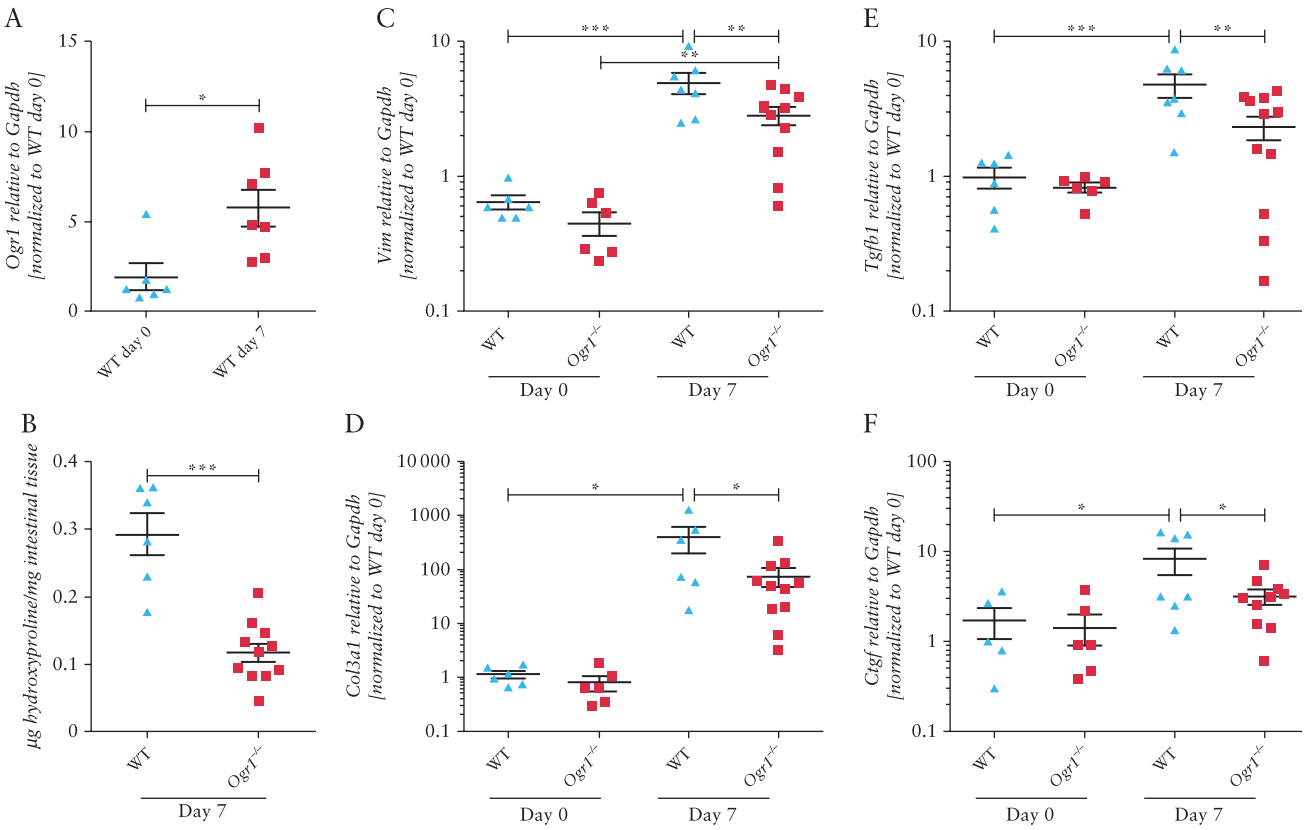

Figure 4. *Ogr1* mRNA expression was significantly increased in WT grafts explanted 7 days after heterotopic transplantation [by unpaired *t*-test, **A**]. HYP content was decreased in grafts from *Ogr1*$^{-/-}$ donor mice explanted on Day 7 after heterotopic transplantation, compared with grafts from WT donor mice [by unpaired *t*-test, **B**]. *Vim* [**C**], *Col3a1* [**D**], *Tgfb1* [**E**], and *Ctgf* [**F**] mRNA expression is significantly decreased in grafts from *Ogr1*$^{-/-}$ mice 7 days after heterotopic transplantation, compared with WT grafts [ANOVA *post-hoc* Newman–Keuls multiple comparison test].

3.7. Collagen deposition was decreased in *Ogr1*$^{-/-}$ grafts after induction of fibrosis

Collagen layer thickness visualized by Sirius Red staining was quantified under transmission light and under polarizing light before and after induction of fibrosis [Figure 5]. Collagen deposition was increased when using terminal ileum from WT mice as grafts (collagen layer thickness 12.44 ± 0.51 µm vs 8.72 ± 0.68 µm, $p < 0.001$ under transmission light [Figure 5A], 10.71 ± 0.41 µm vs 6.80 ± 0.38 µm, $p < 0.001$ under polarized light [Figure 5B]). The collagen layer in the *Ogr1*$^{-/-}$ grafts was significantly increased 7 days after heterotopic transplantation (collagen layer thickness 10.56 ± 0.29 µm vs 7.93 ± 0.47 µm, $p < 0.01$ under transmission light [Figure 5A], 8.71 ± 0.39 µm vs 5.91 ± 0.31 µm, $p < 0.001$ under polarized light [Figure 5B]). Consistent with expression of the fibrosis mRNA, the collagen layer in harvested grafts on Day 7 from *Ogr1*$^{-/-}$ mice was significantly thinner compared with the collagen layer in grafts from WT mice (10.56 ± 0.29 µm vs 12.44 ± 0.51 µm, $p < 0.01$ for data obtained under transmission light [Figure 5A] and 8.71 ± 0.39 µm vs 10.71 ± 0.41 µm, $p < 0.001$ for data obtained under polarized light microscopy [Figure 5B]).

Collagen deposition in the grafts was furthermore quantified by image processing evaluation [color threshold] with ImageJ. Polarized light microscopy showed a significant decrease in collagen layer thickness in grafts from *Ogr1*$^{-/-}$ donor mice compared with in grafts from WT donor mice (0.44 ± 0.06 vs 0.73 ± 0.10, arbitrary units, $p < 0.05$ [Figure 5C]).

4. Discussion

In this study, we demonstrate that expression of the pH-sensing receptor OGR1 correlates with fibrosis in the terminal ileum in mice and humans. When analysing the terminal ileum from patients with CD, we observed increased expression of the pH-sensing GPR *OGR1* in the fibrosis-affected area, compared with the non-fibrotic resection margin. We also found a positive correlation between the expression of markers involved in different phases of fibrosis, e.g. pro-fibrotic cytokines [*TGFB1* and *CTGF*], a marker for activation of myofibroblasts [*ACTA2*], or pro-collagens [*COL1A1* and *COL3A1*], and the expression of *OGR1*. Using an *in vivo* murine model for intestinal fibrosis, we could confirm an increased expression of the pH-sensing receptor *Ogr1* upon fibrogenesis. Furthermore, we demonstrated decreased fibrosis in double knockout mice deficient for *Ogr1* and *Il10* compared with control mice deficient for *Il10* following spontaneous colitis. Additionally, we observed a decrease in fibrosis between *Ogr1*-deficient mice in DSS-induced chronic colitis and WT

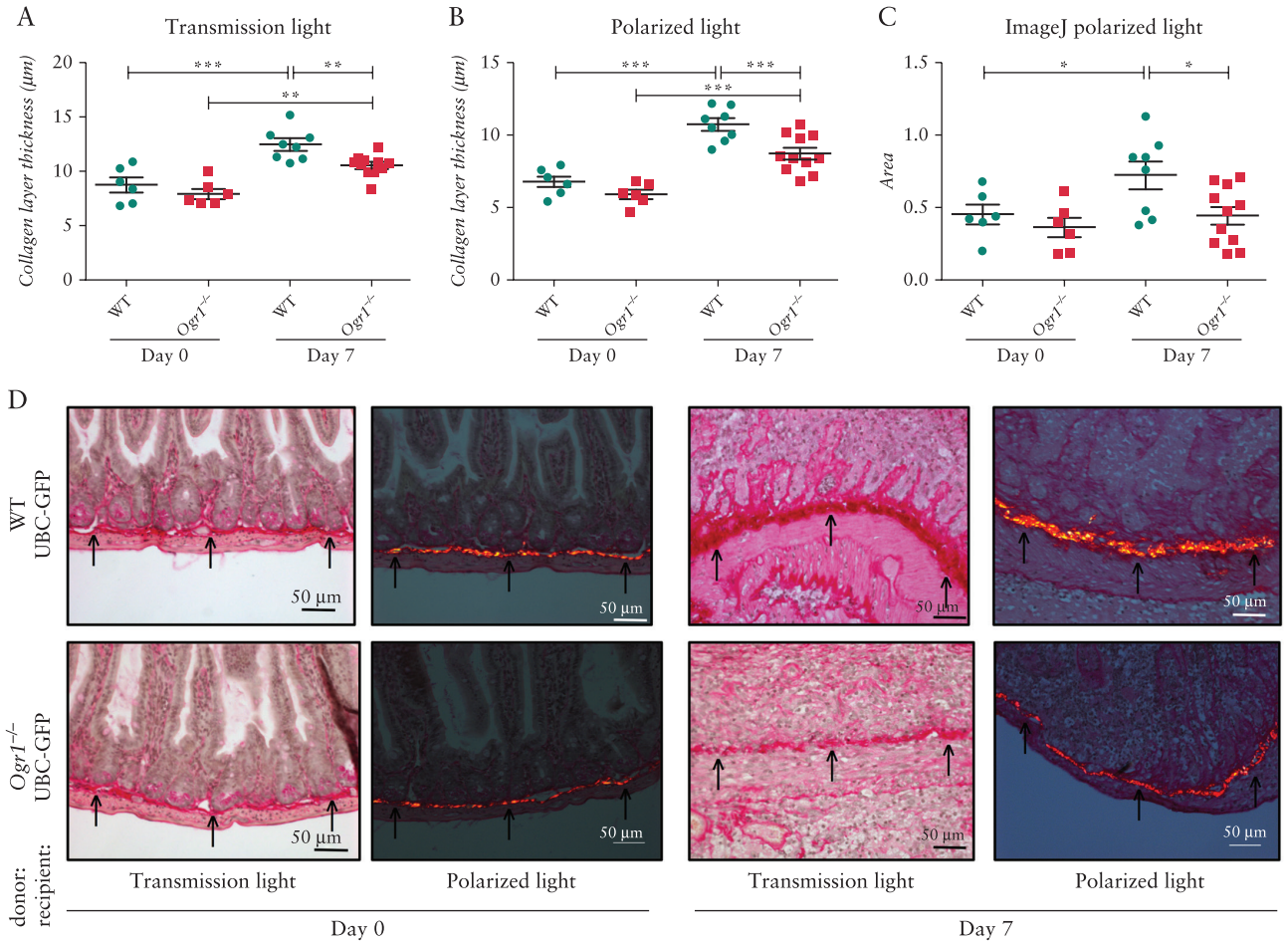

Figure 5. Collagen quantity and collagen layer thickness were significantly decreased in grafts from *Ogr1*$^{-/-}$ donor mice compared with WT donor mice 7 days after heterotopic transplantation. Quantification of collagen layer thickness [µm] by Sirius Red staining with and without polarized light filter [**A+B**], by ANOVA *post-hoc* Newman–Keuls multiple comparison test. Area of collagen deposition stained by Sirius Red and quantified using ImageJ under transmission light [**C**]. Representative pictures of collagen deposition [arrows] visualized using Sirius Red staining with and without polarized light [**D**].

mice. Comparing heterotopic transplantation of terminal ileum from *Ogr1*$^{-/-}$ mice to transplantation of ileum from WT mice, we detected a significant decrease in the mRNA expression of fibrosis markers, as well as a decrease in collagen layer thickness and HYP in the *Ogr1*$^{-/-}$ grafts. These results, from three different well-established murine models of intestinal fibrosis, indicate a role for the pH-sensing receptor OGR1 in fibrogenesis and stricture formation in CD, thereby providing a new target for therapeutic intervention.

Intestinal fibrosis, which typically occurs in the terminal ileum of patients with CD, is triggered as a response to inflammatory processes, in which fibroblasts become activated. Activated myofibroblasts can deposit excessive amounts of ECM proteins as part of the wound-healing process, thereby causing stricture formation.[44] Fibrosis is the result of a disturbance in the balance between ECM formation and matrix metalloproteinase–mediated degradation of ECM proteins.[45] Intestinal inflammation is accompanied by tissue acidification due to the hypoxic environment and the excessive production and insufficient elimination of glycolytic metabolites e.g. lactic acid.[46–48] Local acidification of the gut lumen and mucosa occurs during intestinal inflammation.[46] This indicates that luminal and tissue pH is decreased during active and longstanding IBD, which could activate downstream signalling by pH-sensing receptors. The heterotopic transplantation of intestine resections under the skin induces a cellular, fibrosis-inducing response from the graft as well as from the recipient.[42] The graft is subjected to ischemia, which causes hypoxia and thereby anaerobic glycolysis and production of lactic acid.[15–17] The ensuing decrease in pH may stimulate pH-sensing receptors such as OGR1. Furthermore, hypoxia induces the accumulation of hypoxia-inducible factors [HIFs] and the release of pro-inflammatory cytokines such as TNF and interleukin [IL] 6.[49,50] Only recently have we found that the pH-sensing receptor OGR1 plays a role in IBD and that genetic deletion of *Ogr1* partially prevents the development of colitis in the *IL10*-deficient IBD mouse model.[4] Moreover, the absence of *Gpr4* ameliorating colitis in IBD animal models indicates an important regulatory role of this pH-sensing receptor in mucosal inflammation.[5] Recently, we showed that expression of *Ogr1*, *Tdag8*, *Il6*, and *Tnf* are induced by the combination of hypoxia and extracellular acidosis in WT mouse peritoneal macrophages, but not in peritoneal macrophages from *Ogr1*$^{-/-}$ mice.[50] Inflammatory cells, such as macrophages, release factors that stimulate both fibroblast activation and proliferation, resulting in synthesis and deposition of components of the ECM.[51] We recently showed that acidosis induced OGR1-mediated genes in murine peritoneal macrophages that are associated with adhesion and ECM, and actin cytoskeletal regulation.[4] Additionally, in an intestinal epithelial cell model stably overexpressing OGR1, acidosis stimulated OGR1-mediated genes involved in cell adhesion and cytoskeletal regulatory genes.[3] In conclusion, these studies indicate a pathophysiological role for pH-sensing receptors during the pathogenesis of mucosal inflammation, and provide a new link between tissue pH and immune responses.[4]

pH-dependent signalling is not only relevant for the induction of inflammation, but also for the progression to fibrosis. Links between extracellular acidification and activation of fibroblasts, as well as ECM remodelling via pH-sensing GPCRs have been described before. Zhu et al. demonstrated that differentiation of human bone-marrow–derived mesenchymal stem cells [MSCs] into cancer-associated fibroblasts via OGR1 occurs upon decreasing the extracellular pH to 7.0 *in vitro*. In this study, differentiation of MSCs into myofibroblasts was accompanied by increased protein expression of vimentin and alpha smooth muscle actin [αSMA].[52] Furthermore, Li et al. show that migration of MCF-7 cells [human breast adenocarcinoma cell line] overexpressing OGR1 is decreased [without exposing them to an acidic environment] and that this effect might be mediated via a GTPase Gα 12/13– Rho–Rac1 pathway.[52] Differences in migratory function of intestinal fibroblasts isolated from stricturing and fistulating areas upon activation have been determined as factors in the mechanism of intestinal fibrosis as well. These mechanisms may contribute to the induction of fibrosis in this model, and explain the reduced fibrotic processes in grafts from *Ogr1*$^{-/-}$ mice.[53]

OGR1 is also involved in tissue remodelling in severe asthma and irreversible airway obstruction.[54] Airway remodelling results from increased expression of connective tissue or extracellular matrix proteins, airway smooth muscle cells [ASMCs] hyperplasia, and hypertrophy.[55] The process is associated with airway acidification in asthma.[56] Extracellular acidication results in the induction of connective tissue growth factor expression. This can be prevented by inhibiting *OGR1* with small interfering RNA and protein-specific inhibitors.[54] Additionally, Saxena et al. described how the activation of *OGR1* in human ASMC by decreasing the extracellular pH to 6.8 causes contraction and cell stiffness, which was attenuated by *OGR1* silencing.[57]

There is evidence that intestinal fibrogenesis is self-perpetuating,[58] and that once initiated, its progression may not depend on the presence of inflammation but on persisting mucosal acidification.[59] Administration of anti-inflammatory agents effectively treats inflammatory flares, but may not prevent intestinal fibrosis.[60,61]

In conclusion, we have provided the first evidence that OGR1 plays a role in intestinal fibrosis. *Ogr1* deficiency leads to a significant decrease in mRNA expression of fibrosis markers, as well as an evident reduction in collagen deposition in our models for intestinal fibrosis. A decrease in HYP content after induction of fibrosis suggests that also stabilization of collagen is impaired in grafts from *Ogr1*$^{-/-}$ compared with WT. The relevance of these findings is extended by the positive correlation between the expression of *OGR1* and fibrosis markers in human ileum affected with fibrosis in CD patients. Increased expression of OGR1 triggered by inflammation-associated acidification, and subsequent cellular responses might perpetuate inflammation-induced fibrosis in IBD. The presence of OGR1 in human and murine intestinal tissue is associated with fibrosis, making it a potential future target for treatment for IBD-associated fibrogenesis.

Funding

This research was supported by a research grant FreeNovation from Novartis to MH, by a research grant [grant number: 314730_152895 / 1] from the Swiss National Science Foundation to MH, by a grant from the Swiss National Science Foundation [grant number 31003A_155959] to CAW, and by a grant from the Swiss National Science Foundation to BM [grant No. 32473B_156525]. PHIS was a recipient of a Junior Grant from the National Center of Competence in Research [NCCR Kidney] [CH] funded by the Swiss National Science Foundation.

Conflict of Interest

GR discloses grant support from AbbVie, Ardeypharm, MSD, FALK, Flamentera, Novartis, Roche, Tillots, UCB, and Zeller. MH discloses grant support from AbbVie and Novartis. GD discloses unrestricted grants: Abbvie, Takeda; advisory boards: Mundipharma, Pharmacosmos; speakers' fees: Takeda, Janssen pharmaceuticals. BM discloses a research grant from MSD; advisory board membership: Gilead, Novigenix; speakers' fees: MSD.

SH, WTvH, AH, KB, NH, TR, CM, BM, BW, CM, CdV, AW, PHIS, CAW, IFW, and PAR have no conflict of interest to disclose.

Acknowledgments

No external writing assistance was provided in drafting this manuscript. The manuscript, including related data, figures and tables has not been previously published and the manuscript is not under consideration elsewhere.

Author Contributions

GR: study concept.
SH, WTvH, MH: acquisition of data and drafting of the manuscript.
AH, CM, BW, CFM, KB, NH, PHIS: acquisition of data.
BM, GR, GD, CdV, AW, CW, IF-W, PAR, MH: critical revision of the manuscript.
CM, TR: technical support.
All authors approved the final submitted version of the manuscript.

Supplementary Data

Supplementary data are available at *ECCO-JCC* online.

References

1. Franke A, McGovern DP, Barrett JC, *et al.* Genome-wide meta-analysis increases to 71 the number of confirmed Crohn's disease susceptibility loci. *Nat Genet* 2010;**42**:1118–25.
2. Jostins L, Ripke S, Weersma RK, *et al.*; International IBD Genetics Consortium [IIBDGC]. Host–microbe interactions have shaped the genetic architecture of inflammatory bowel disease. *Nature* 2012;**491**:119–24.
3. de Vallière C, Vidal S, Clay I, *et al.* The pH-sensing receptor OGR1 improves barrier function of epithelial cells and inhibits migration in an acidic environment. *Am J Physiol Gastrointest Liver Physiol* 2015;**309**:G475–90.
4. de Vallière C, Wang Y, Eloranta JJ, *et al.* G Protein-coupled pH-sensing receptor OGR1 is a regulator of intestinal inflammation. *Inflamm Bowel Dis* 2015;**21**:1269–81.
5. Wang Y, de Vallière C, Imenez Silva PH, *et al.* The proton-activated receptor GPR4 modulates intestinal inflammation. *J Crohns Colitis* 2018;**12**:355–68.
6. Seuwen K, Ludwig MG, Wolf RM. Receptors for protons or lipid messengers or both? *J Recept Signal Transduct Res* 2006;**26**:599–610.
7. Ludwig MG, Vanek M, Guerini D, *et al.* Proton-sensing G-protein-coupled receptors. *Nature* 2003;**425**:93–8.
8. Venkatakrishnan AJ, Deupi X, Lebon G, Tate CG, Schertler GF, Babu MM. Molecular signatures of G-protein-coupled receptors. *Nature* 2013;**494**:185–94.
9. Heng BC, Aubel D, Fussenegger M. An overview of the diverse roles of G-protein coupled receptors [GPCRs] in the pathophysiology of various human diseases. *Biotechnol Adv* 2013;**31**:1676–94.
10. Chini B, Parenti M, Poyner DR, Wheatley M. G-protein-coupled receptors: From structural insights to functional mechanisms. *Biochem Soc Trans* 2013;**41**:135–6.
11. Wang JQ, Kon J, Mogi C, *et al.* TDAG8 is a proton-sensing and psychosine-sensitive G-protein-coupled receptor. *J Biol Chem* 2004;**279**:45626–33.
12. Ishii S, Kihara Y, Shimizu T. Identification of T cell death-associated gene 8 [TDAG8] as a novel acid sensing G-protein-coupled receptor. *J Biol Chem* 2005;**280**:9083–7.
13. Mogi C, Tobo M, Tomura H, *et al.* Involvement of proton-sensing TDAG8 in extracellular acidification-induced inhibition of proinflammatory cytokine production in peritoneal macrophages. *J Immunol* 2009;**182**:3243–51.
14. Radu CG, Nijagal A, McLaughlin J, Wang L, Witte ON. Differential proton sensitivity of related G protein-coupled receptors T cell death-associated gene 8 and G2A expressed in immune cells. *Proc Natl Acad Sci U S A* 2005;**102**:1632–7.
15. Lardner A. The effects of extracellular pH on immune function. *J Leukoc Biol* 2001;**69**:522–30.
16. Park SY, Bae DJ, Kim MJ, Piao ML, Kim IS. Extracellular low pH modulates phosphatidylserine-dependent phagocytosis in macrophages by increasing stabilin-1 expression. *J Biol Chem* 2012;**287**:11261–71.
17. Simmen HP, Battaglia H, Giovanoli P, Blaser J. Analysis of pH, pO2 and pCO2 in drainage fluid allows for rapid detection of infectious complications during the follow-up period after abdominal surgery. *Infection* 1994;**22**:386–9.
18. Hanly EJ, Aurora AA, Shih SP, *et al.* Peritoneal acidosis mediates immunoprotection in laparoscopic surgery. *Surgery* 2007;**142**:357–64.
19. Brokelman WJ, Lensvelt M, Borel Rinkes IH, Klinkenbijl JH, Reijnen MM. Peritoneal changes due to laparoscopic surgery. *Surg Endosc* 2011;**25**:1–9.
20. Mohebbi N, Benabbas C, Vidal S, *et al.* The proton-activated G protein coupled receptor OGR1 acutely regulates the activity of epithelial proton transport proteins. *Cell Physiol Biochem* 2012;**29**:313–24.
21. Pardo A, Selman M. Matrix metalloproteases in aberrant fibrotic tissue remodeling. *Proc Am Thorac Soc* 2006;**3**:383–8.
22. Kim H, Oda T, López-Guisa J, *et al.* TIMP-1 deficiency does not attenuate interstitial fibrosis in obstructive nephropathy. *J Am Soc Nephrol* 2001;**12**:736–48.
23. Underwood DC, Osborn RR, Bochnowicz S, *et al.* SB 239063, a p38 MAPK inhibitor, reduces neutrophilia, inflammatory cytokines, MMP-9, and fibrosis in lung. *Am J Physiol Lung Cell Mol Physiol* 2000;**279**:L895–902.
24. Vaillant B, Chiaramonte MG, Cheever AW, Soloway PD, Wynn TA. Regulation of hepatic fibrosis and extracellular matrix genes by the Th response: New insight into the role of tissue inhibitors of matrix metalloproteinases. *J Immunol* 2001;**167**:7017–26.
25. Speca S, Giusti I, Rieder F, Latella G. Cellular and molecular mechanisms of intestinal fibrosis. *World J Gastroenterol* 2012;**18**:3635–61.
26. Rieder F, Fiocchi C, Rogler G. Mechanisms, management, and treatment of fibrosis in patients with inflammatory bowel diseases. *Gastroenterology* 2017;**152**:340–350.e6.
27. Latella G, Di Gregorio J, Flati V, Rieder F, Lawrance IC. Mechanisms of initiation and progression of intestinal fibrosis in IBD. *Scand J Gastroenterol* 2015;**50**:53–65.
28. Latella G, Rogler G, Bamias G, *et al.* Results of the 4th scientific workshop of the ECCO [I]: pathophysiology of intestinal fibrosis in IBD. *J Crohns Colitis* 2014;**8**:1147–65.
29. Lawrance IC, Rogler G, Bamias G, *et al.* Cellular and molecular mediators of intestinal fibrosis. *J Crohns Colitis* 2017;**11**:1491–1503.
30. Li C, Flynn RS, Grider JR, *et al.* Increased activation of latent TGF-β1 by αVβ3 in human Crohn's disease and fibrosis in TNBS colitis can be prevented by cilengitide. *Inflamm Bowel Dis* 2013;**19**:2829–39.
31. Li C, Iness A, Yoon J, *et al.* Noncanonical STAT3 activation regulates excess TGF-β1 and collagen I expression in muscle of stricturing Crohn's disease. *J Immunol* 2015;**194**:3422–31.
32. Scarpa M, Bortolami M, Morgan SL, *et al.* TGF-beta1 and IGF-1 and anastomotic recurrence of Crohn's disease after ileo-colonic resection. *J Gastrointest Surg* 2008;**12**:1981–90.
33. Del Zotto B, Mumolo G, Pronio AM, Montesani C, Tersigni R, Boirivant M. TGF-beta1 production in inflammatory bowel disease: Differing production patterns in Crohn's disease and ulcerative colitis. *Clin Exp Immunol* 2003;**134**:120–6.
34. de Bruyn JR, Meijer SL, Wildenberg ME, Bemelman WA, van den Brink GR, D'Haens GR. Development of fibrosis in acute and longstanding ulcerative colitis. *J Crohns Colitis* 2015;**9**:966–72.
35. Cosnes J, Cattan S, Blain A, *et al.* Long-term evolution of disease behavior of Crohn's disease. *Inflamm Bowel Dis* 2002;**8**:244–50.
36. Freeman HJ. Natural history and clinical behavior of Crohn's disease extending beyond two decades. *J Clin Gastroenterol* 2003;**37**:216–9.
37. Ippolito C, Colucci R, Segnani C, *et al.* Fibrotic and vascular remodelling of colonic wall in patients with active ulcerative colitis. *J Crohns Colitis* 2016;**10**:1194–204.
38. Grossmann J, Walther K, Artinger M, *et al.* Progress on isolation and short-term *ex-vivo* culture of highly purified non-apoptotic human intestinal epithelial cells [IEC]. *Eur J Cell Biol* 2003;**82**:262–70.

39. Obermeier F, Kojouharoff G, Hans W, Schölmerich J, Gross V, Falk W. Interferon-gamma [IFN-gamma]- and tumour necrosis factor [TNF]-induced nitric oxide as toxic effector molecule in chronic dextran sulphate sodium [DSS]-induced colitis in mice. *Clin Exp Immunol* 1999;**116**:238–45.
40. Becker C, Fantini MC, Wirtz S, *et al.* *In vivo* imaging of colitis and colon cancer development in mice using high resolution chromoendoscopy. *Gut* 2005;**54**:950–4.
41. Steidler L, Hans W, Schotte L, *et al.* Treatment of murine colitis by *Lactococcus lactis* secreting interleukin-10. *Science* 2000;**289**:1352–5.
42. Hausmann M, Rechsteiner T, Caj M, *et al.* A new heterotopic transplant animal model of intestinal fibrosis. *Inflamm Bowel Dis* 2013;**19**:2302–14.
43. Rittié L. Method for picrosirius red-polarization detection of collagen fibers in tissue sections. *Methods Mol Biol* 2017;**1627**:395–407.
44. Rieder F, Fiocchi C. Intestinal fibrosis in IBD—a dynamic, multifactorial process. *Nat Rev Gastroenterol Hepatol* 2009;**6**:228–35.
45. van Haaften WT, Mortensen JH, Karsdal MA, Bay-Jensen AC, Dijkstra G, Olinga P. Misbalance in type III collagen formation/degradation as a novel serological biomarker for penetrating [Montreal B3] Crohn's disease. *Aliment Pharmacol Ther* 2017;**46**:26–39.
46. Fallingborg J, Christensen LA, Jacobsen BA, Rasmussen SN. Very low intraluminal colonic pH in patients with active ulcerative colitis. *Dig Dis Sci* 1993;**38**:1989–93.
47. Nugent SG, Kumar D, Rampton DS, Evans DF. Intestinal luminal pH in inflammatory bowel disease: possible determinants and implications for therapy with aminosalicylates and other drugs. *Gut* 2001;**48**:571–7.
48. Press AG, Hauptmann IA, Hauptmann L, *et al.* Gastrointestinal pH profiles in patients with inflammatory bowel disease. *Aliment Pharmacol Ther* 1998;**12**:673–8.
49. Bartels K, Grenz A, Eltzschig HK. Hypoxia and inflammation are two sides of the same coin. *Proc Natl Acad Sci U S A* 2013;**110**:18351–2.
50. de Vallière C, Cosin-Roger J, Simmen S, *et al.* Hypoxia positively regulates the expression of pH-sensing G-protein-coupled receptor OGR1 [GPR68]. *Cell Mol Gastroenterol Hepatol* 2016;**2**:796–810.
51. Kumagai S, Ohtani H, Nagai T, *et al.* Platelet-derived growth factor and its receptors are expressed in areas of both active inflammation and active fibrosis in inflammatory bowel disease. *Tohoku J Exp Med* 2001;**195**:21–33.
52. Zhu H, Guo S, Zhang Y, *et al.* Proton-sensing GPCR–YAP signalling promotes cancer-associated fibroblast activation of mesenchymal stem cells. *Int J Biol Sci* 2016;**12**:389–96.
53. Meier JK, Scharl M, Miller SN, *et al.* Specific differences in migratory function of myofibroblasts isolated from Crohn's disease fistulae and strictures. *Inflamm Bowel Dis* 2011;**17**:202–12.
54. Matsuzaki S, Ishizuka T, Yamada H, *et al.* Extracellular acidification induces connective tissue growth factor production through proton-sensing receptor OGR1 in human airway smooth muscle cells. *Biochem Biophys Res Commun* 2011;**413**:499–503.
55. Vignola AM, Kips J, Bousquet J. Tissue remodeling as a feature of persistent asthma. *J Allergy Clin Immunol* 2000;**105**:1041–53.
56. Kodric M, Shah AN, Fabbri LM, Confalonieri M. An investigation of airway acidification in asthma using induced sputum: A study of feasibility and correlation. *Am J Respir Crit Care Med* 2007;**175**:905–10.
57. Saxena H, Deshpande DA, Tiegs BC, *et al.* The GPCR OGR1 [GPR68] mediates diverse signalling and contraction of airway smooth muscle in response to small reductions in extracellular pH. *Br J Pharmacol* 2012;**166**:981–90.
58. Johnson LA, Luke A, Sauder K, *et al.* Intestinal fibrosis is reduced by early elimination of inflammation in a mouse model of IBD: Impact of a "Top-Down" approach to intestinal fibrosis in mice. *Inflamm Bowel Dis* 2012;**18**:460–71.
59. Rieder F, Kessler S, Sans M, Fiocchi C. Animal models of intestinal fibrosis: New tools for the understanding of pathogenesis and therapy of human disease. *Am J Physiol Gastrointest Liver Physiol* 2012;**303**:G786–801.
60. D'Haens G, Geboes K, Rutgeerts P. Endoscopic and histologic healing of Crohn's [ileo-] colitis with azathioprine. *Gastrointest Endosc* 1999;**50**:667–71.
61. Vermeire S, van Assche G, Rutgeerts P. Review article: Altering the natural history of Crohn's disease—evidence for and against current therapies. *Aliment Pharmacol Ther* 2007;**25**:3–12.